Jonathan Decker (Autor)

# Investigation of monolithically integrated spectral stabilization in high-brightness broad area diode lasers

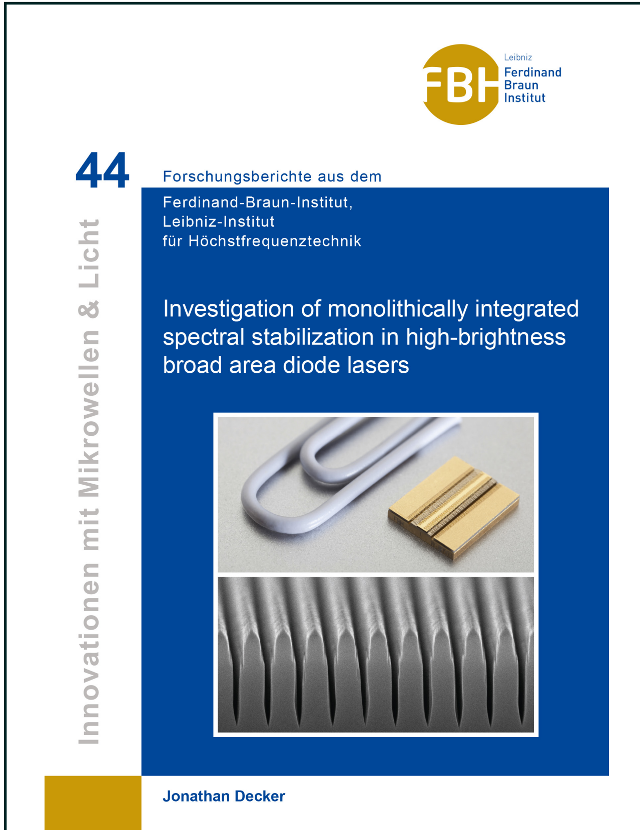


https://cuvillier.de/de/shop/publications/7814

Copyright:
Cuvillier Verlag, Inhaberin Annette Jentzsch-Cuvillier, Nonnenstieg 8, 37075 Göttingen, Germany
Telefon: +49 (0)551 54724-0, E-Mail: info@cuvillier.de, Website: https://cuvillier.de

# 1. Introduction

## 1.1. Motivation

Nowadays, laser diodes are key components in systems for material processing, optical communication, medical applications and sensing [1, 2]. In comparison to solid state, gas and fiber lasers, direct diode laser (DDL) systems, which combine the output of many laser diodes and arrays into one beam, deliver high output powers with the highest conversion efficiency at low costs. Other advantages of DDLs are the small footprint, the wide addressable wavelength range, and the long term reliability. However, high power DDLs suffer from a relatively poor beam quality limiting the brightness, which is a measure for the optical peak-intensity of the output. Although in the past decades high-power diode lasers have emerged as indispensable tools for all kinds of low-brightness industrial applications like welding, brazing, soldering and printing [3], high-brightness applications like sheet-metal cutting were inaccessible for DDLs [4]. In Figure 1.1 the brightness of DDLs in comparison to gas and solid state lasers, which is proportional to output power per beam parameter product (BPP, cf. section 2.4), is illustrated [5]. To overcome the lack of brightness of DDL systems diode lasers are currently most commonly used as pump sources for solid

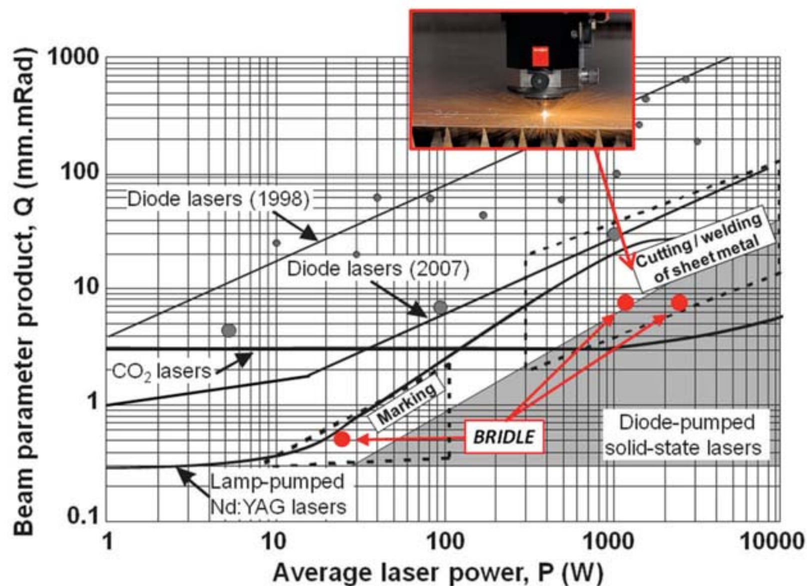


**Fig. 1.1.:** Beam quality in terms of BPP versus output power for high-power for gas, solid state, and diode lasers, adapted from [5].

Dieses Werk ist copyrightgeschützt und darf in keiner Form vervielfältigt werden noch an Dritte weitergegeben werden.
Es gilt nur für den persönlichen Gebrauch.

state and fiber lasers that operate as a brightness converters and can deliver diffraction limited output [6]. As the improvement of brightness in diode pumped solid state lasers (DPSSL) comes with a deterioration in wall-plug efficiency, and an increase in cost and setup complexity, it has been a crucial goal to further increase the brightness of DDLs. Recently, significantly improved brightness from DDL system has been reported by several groups and companies [7, 8, 9, 10, 11]. The key-drivers in the improvement are spectral beam combining (SBC) techniques, in which the emission of many spectrally stabilized laser diodes is spatially superimposed using spectrally selective elements (e.g. diffractive gratings). In contrast to conventional DDL systems where laser arrays are optically stacked in one or two dimensions and the brightness scales with the brightness of a single array elements, DDL systems based on SBC-techniques allow to scale the brightness additionally with the number of combined wavelengths [12]. The maximal brightness-scaling is achieved when each emitter is stabilized to a unique wavelength with narrow linewidth and the spacing between the wavelength channels is as dense as possible. These concepts, termed as *dense spectral beam combining* (DSBC) or *dense wavelength division multiplexing* (DWDM), are in wide use in optical communication networks [13, 14, 15, 16], and are recently making their way into high-power DDLs. In current setups the spectral stabilization and combining is achieved most commonly via an external cavity. Although spectral stabilization can be realized externally, it adds cost, increases size and setup complexity [8], and is sensible to mechanical pertubations. Further, external optical feedback is increased, which is known to cause mode instabilities [17] and emitter failures [18, 19, 20], even though some groups report successful mitigation of these failures e.g. by better alignment of the optical elements and smile compensation [21]. To mitigate these drawbacks alternative approaches for more compact, low-cost modules based on monolithic spectral stabilization of laser diodes are developed within the EU-funded BRIDLE project (`www.bridle.eu`). The success of a monolithic approach toward spectral stabilization of high-power laser diodes will depend heavily on the available possibilities to mitigate the degradation in electro-optical performance in comparison to unstabilized Fabry-Pérot lasers, while a sufficient narrow and stable spectrum is achieved.

## 1.2. State of the art

AlGaAs based high-power broad area (BA) lasers in Fabry-Pérot (FP) configuration are the most efficient light-sources for converting electrical input into optical output power, with wallplug efficiencies $> 70\%$ [22, 23]. State of the art BA lasers have a stripe width of $W$ = 90-100 $\mu$m and emit at $\lambda$ = 910-980 nm delivering output powers of P $\geq$ 10 W with an operating conversion efficiency of $\eta_E \approx 65\%$ [24]. Maximal output powers of up to P = 25 W in continuous wave operation have been reported in [25, 26], when light is coupled out at one facet, and P $\approx$ 30 W, when light is coupled out from both facets simultanously [27]. At high current and output levels (P = 10 W) BA laser operate with an in-plane BPP of 3-4 mm$\times$mrad [28]. First realizations of monolithic spectral stabilization in high-power (P $\geq$ 1 W) broad area lasers have been reported in 1998 from Earles *et al.* [29], where P = 1.1 W with $\eta_E = 32\%$ was achieved, using buried overgrown distributed feedback (DFB) gratings. While a chronological overview of the developement of spectrally stabilized high-power DFB-BA lasers is given here in Table 1.1, the author refers to [30] for a more general review of monolithic spectral stabilization in high-power diode



Dieses Werk ist copyrightgeschützt und darf in keiner Form vervielfältigt werden noch an Dritte weitergegeben werden.
Es gilt nur für den persönlichen Gebrauch.

| author | year | lasertype | fabrication | $W$ [$\mu$m] | $\lambda$ [nm] | $\Delta\lambda_{FWHM}$ [nm] | $P$ [W] | $\eta_{E,max}$ [%] |
|---|---|---|---|---|---|---|---|---|
| Earles [29] | 1998 | DFB | overgrowth | 100 | 893 | 0.1 | 1.1 | 32 |
| Chang [31] | 2000 | DFB | overgrowth | 100 | 976 | 0.15 | 1.0 | 33 |
| Klehr [32] | 2006 | DFB | overgrowth | 100 | 808 | 0.1 | 4.7 | 38 |
| Kanskar [33] | 2006 | DFB | overgrowth | 100 | 975 | 0.2 | 5.5 | 53 |
| He [34] | 2009 | DFB | overgrowth | 100 | 808 | 0.3 | 4.0 | 57 |
| Schultz [35] | 2010 | DFB | overgrowth | 90 | 976 | 0.4 | 11.0 | 58 |
| Crump [36] | 2012 | DFB | overgrowth | 90 | 975 | $0.7^{a}$ | 10.0 | 62 |
| Fricke [37] | 2012 | DFB | surface etching | 90 | 976 | 0.5 | 10.0 | 51 |
| Decker [38] | 2014 | DFB | surface etching | 30 | 970 | $0.7^{a}$ | 6.7 | 54 |
| Decker [39] | 2015 | DFB-array | surface etching | 30 | 975 | $0.8^{a}$ | 5.0 | 48 |
| Decker [40] | 2016 | DFB-array | surface etching | 30 | 975 | $0.9^{a}$ | 5.6 | 56 |

**Tab. 1.1.:** Chronological developement of high-power (P $\geq$ 1 W, cw) DFB-BA lasers. The last three publications can be considered as the fundamentals of this work ($^{a}$*linewidth with 95% power content is given*).

lasers. In the following years output power and efficiency were increased up to 5.5 W with peak conversion efficiencies up to $\eta_E = 57\%$ [31, 32, 33, 34]. Latest progress has been reported by Schultz *et al.* in 2011 and 2012, respectively, with P = 11 W and a peak conversion efficiency of 59% ( $\sim$ 45% at 11 W) in [35], and P > 10 W and peak conversion efficiency of 62% ( $\sim$ 58% at 10 W) in [36]. The significant performance improvement reported in [35] and [36] was driven by two key-achievements, treated in detail in [41]: Firstly, a numerical model based on the coupled mode theory (CMT) was developed, that allowed to identify grating configurations with the lowest possible coupling coefficient $\kappa$ to enable spectral stabilization without lasing in FP-modes. Secondly, the ability to manufacture and implement the designed grating configurations into the laser diode without introducing significant amounts of additional optical and electrical losses, was developed. Note that the achieved performance of DFB-BA lasers in [36] is comparable to the performance of spectrally unstabilized FP-BA lasers. Although BA lasers with buried DFB gratings show excellent performance in spectral stability, output power and conversion efficiency, they have a couple of disadvantages due to the interruption of epitaxial growth, that can lead to oxygen-contamination and crystal defects [42] as well as partial variations in material composition [43]. An alternative monolithic approach is the etching of high order gratings directly into the p-side surface of the BA lasers, where the interruption of epitaxial growth is omitted. A proof of principle for high-power BA lasers was reported from the group of Fricke *et al.* for DBR-BA lasers in [44, 45], where up to P = 14 W and 50% peak efficiency have been achieved, as well as for DFB-BA lasers, where up to P = 11 W and 50% peak efficiency have been achieved [37]. For high-power DFB-BA lasers with buried gratings the limitations of output power and conversion efficiency have been studied extensively (cf. [36] and the references therein). However, the limitations of conversion efficiency and output power in high-power DFB lasers with surface etched gratings have not been fully understood at the beginning of this work. This is mainly attributed



Dieses Werk ist copyrightgeschützt und darf in keiner Form vervielfältigt werden noch an Dritte weitergegeben werden.
Es gilt nur für den persönlichen Gebrauch.

to the fact that surface etched gratings introduce a high index contrast into the cavity and can therefore not be calculated directly within the coupled mode theory [46, 47]. Further, only limited information are available on the influence of monolithic integrated gratings on the beam quality in highly efficient DFB-BA lasers.

## 1.3. Goal of this work

The goal of this work is to contribute to a better understanding of the theoretical and technical limitations of conversion efficiency and output power in high-power DFB-BA lasers with surface etched gratings. That includes the analysis of scattering losses and coupling coefficient $\kappa$, and how they are influenced by e.g. the groove geometry, etching depth and grating order or epitaxial layer structure to understand limitations and identify reasons for device degradation. Therefore the model based on CMT presented in [41] is used as starting point and extended to gratings with high index contrast, by using a bidirectional eigenmode expansion and propagation method for the calculation of an effective coupling coefficient and radiation losses of a surface etched grating. Results of the simulation are compared comprehensively to experimental data from diagnostic DFB lasers and their Fabry-Pérot counterparts.

Another goal of this work is to demonstrate the realization of technically relevant high-power DFB-BA lasers with low BPP for the use in a proof of principal setup for DSBC. The technical framework for the development of such DFB laser arrays is set by the EU granted project BRIDLE (`www.bridle.eu`), where the following specifications (per emitter) are targeted[1]:

- P = 6 W cw output power
- $\Delta\lambda_{95\%} \leq 1$ nm spectral line width (95% power content)
- $\eta_E \geq 50\%$ conversion efficiency (at P = 6 W)
- in-plane $BPP_{lat} \leq 2.0$ mm×mrad (at P = 6 W)

For the use in the DSBC setup spectrally stabilized arrays composed out of five laser diodes are required, comparable to arrays in telecomunication modules [15, 48]. Each emitter should lase at a unique wavelength with a channel spacing of $\Delta\lambda_{CS} = 2.0 - 2.5$ nm around the central wavelength of $\lambda = 975$ nm. Currently $\Delta\lambda_{CS}$ is mainly limited by the properties of the dielectric filter arrays [49] and by $\Delta\lambda_{95\%}$. Note, that this specification cannot be tackled with holographic definition of the grating grooves, but requires I-line or electron beam lithography. To avoid thermal cross talk between the emitters on the array and simplify subsequent optical beam shaping a pitch of 1 mm is required. Figure 1.2 shows a concept for the application of the spectrally stabilized arrays in a DSBC setup using dielectric mirror arrays to superimpose the light of each emitter into one beam. To tackle the technical required specifications for in-plane $BPP_{lat}$, power and conversion efficiency simultaneously, surface etched gratings are studied and realized in lasers with high-brightness narrow stripe broad area (NBA) geometry (W = 30 $\mu$m and L = 6 mm) [50, 23].

[1] Definitions of $\Delta\lambda_{95\%}$, $\eta_E$ and $BPP_{lat}$ can be found in chapter 2



Dieses Werk ist copyrightgeschützt und darf in keiner Form vervielfältigt werden noch an Dritte weitergegeben werden.
Es gilt nur für den persönlichen Gebrauch.

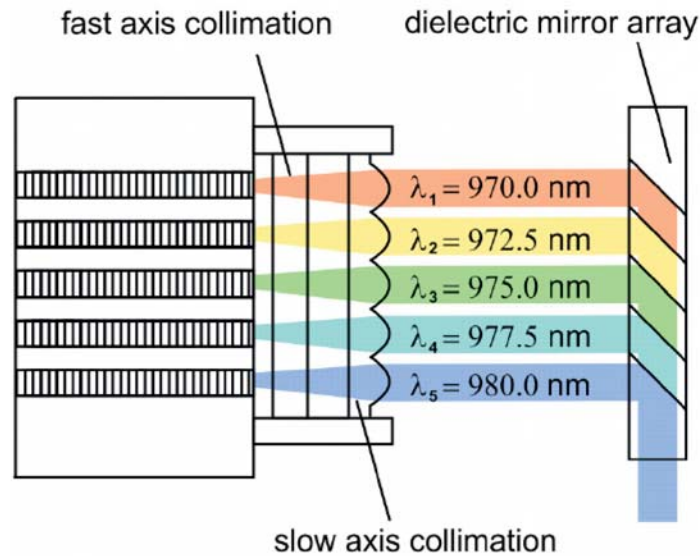


**Fig. 1.2.:** Schematic depiction of DSBC-setup using dielectric filter arrays to combine five spectrally stabilized emitters on a mini-array, each lasing at a unique wavelength around 970-980 nm.

The work is structured as follows: In chapter 2 the theoretical background of high-power diode lasers is introduced, restricted to the most relevant theories and definitions that are indispensable for the understanding of factors limiting the output power, conversion efficiency, brightness and spectral properties of edge emitting BA lasers. In chapter 3 the experimental setup for the laser diode characterization and the corresponding measurement errors are presented. chapter 4 treats the selection of an adequate epitaxial layer structure for the implementation of surface etched gratings in lasers with NBA geometry, based on Fabry-Pérot lasers. Specific challenges for NBA geometry and the resulting requirements to the epitaxial layer structure are discussed. Further the influence of the stripe geometry on in-plane beam quality, output power and conversion efficiency is studied experimentally, based on a comprehensive comparison of FP-BA lasers to FP-NBA lasers. In chapter 5 the numerical model for the simulation of surface etched DFB gratings namely CMT and eigenmode expansion and propagation are introduced. Further, the manufacturing of surface etched gratings is explained. Within three iterations DFP-NBA lasers and arrays are designed, fabricated and experimentally tested. On the way toward improved device performance the influence of the groove geometry, etching depth and grating order on the performance of DFB-NBA lasers is assessed and compared to numerical predictions. All results are summarized in chapter 6, followed by a brief outlook.



Dieses Werk ist copyrightgeschützt und darf in keiner Form vervielfältigt werden noch an Dritte weitergegeben werden.
Es gilt nur für den persönlichen Gebrauch.

Dieses Werk ist copyrightgeschützt und darf in keiner Form vervielfältigt werden noch an Dritte weitergegeben werden.
Es gilt nur für den persönlichen Gebrauch.

# 2. Theoretical foundation of efficient high-brightness diode lasers

Within this chapter the theoretical background of high-power diode lasers is introduced. The understanding of diode lasers requires knowledge in several fields of physics and there is plenty of good literature treating it. A basic understanding of the underlying physics, material systems, and fabrication methods is presumed but the author encourages the reader to look up topics and definitions that are not extensively treated within this chapter or even out of its scope. For example the author refers to [51] for a general introduction into solid state physics, to [52] and [53] for theoretical background of semiconductor lasers and integrated circuits, to [54] and [55] (and the chapters therein e.g. [56] and [57]) for device engineering and diagnostics of diode lasers, and to [5] for an review on diode lasers and diode laser systems with emphasis on their applications.

The topics within this chapter are restricted to the most relevant theories and definitions that are indispensable for the understanding of limitations in high-power diode lasers regarding their conversion efficiency, output power, brightness and spectral properties. The chapter starts with a brief introduction into $Al_xGa_{1-x}As$ based diode lasers (section 2.1), followed by the derivation of lasing threshold, output power and conversion efficiency (including their respective temperature-dependencies). In section 2.2 a numerical model to simulate the performance of broad area lasers is presented and the influence of several characteristic parameters on the device performance is discussed. The spectral properties of material gain and the principles of spectral stabilization are discussed briefly in section 2.3, followed by fundamental definitions of spatial beam quality and brightness (section 2.4). Finally some general concepts of resonator designs for the realization of edge-emitting high-brightness high-power diode lasers are introduced in section 2.6, followed by incoherent beam combining methods for power and brightness scaling, as they are used in complete diode laser systems.

## 2.1. Introduction to AlGaAs/InGaAs based diode lasers

A diode laser is an opto-electronical device, that generates light by stimulated emission from a current-pumped semiconductor as gain medium. The stimulated emission is triggered by recombination of electrons from the conduction band and holes from the valence band at a pn-junction, formed by p-doped and n-doped regions. Relative to the pn-junction plane the following lateral, longitudinal and vertical axes are defined (cf. Figure 2.1) with the same nomenclature being used throughout this work. The most efficient operation at room temperatures has been demonstrated using separate confinement heterostructures (SCH) enabling separate confinement of photons (optical confinement) and carriers (electrical confinement). SCHs are composed of an undoped (intrinsic) low band gap quantum well (QW) serving as a trap for electrons and holes

Dieses Werk ist copyrightgeschützt und darf in keiner Form vervielfältigt werden noch an Dritte weitergegeben werden.
Es gilt nur für den persönlichen Gebrauch.

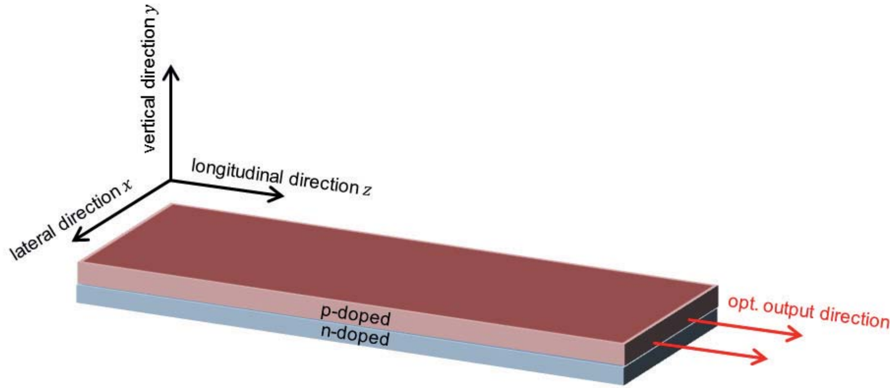


**Fig. 2.1.:** Definition of lateral, longitudinal and vertical axes regarding the pn-junction plane of an edge emitting diode laser used within this work.

sandwiched by p-doped and n-doped high band gap layers (waveguide), enabling carrier confinement. The electrical confinement layers in the middle are sandwiched by p-doped and n-doped layers with a higher refractive index (cladding), respectively, to form a vertical waveguide with optical confinement. Figure 2.2 (a) shows a schematic depiction of band diagramm, refractive index profile and optical intensity profile of a SCH in vertical direction. Note that in typical diode lasers the refractive index is often graded along the waveguides and layers (GRIN-SCH) [58]. Efficient electron-hole-recombination requires very high carrier densities $N_c$ within the QW, most easily achieved at low currents using a thin quantum well. Typical thicknesses are 5-10 nm, which is comparable to the De Broglie wavelength of the electrons and holes. The QW-layers do not require full lattice matching for defect free epitaxial growth, enabling the selection of materials with a wide range of band gap energies, and thus emission wavelengths. Further, strained QW-layers lead to energetic seperation of light holes (providing gain for transversal magnetic (TM) polarization with the vertical electric field vector parallel to the QW) and heavy holes (providing gain for transversal electric (TE) polarization with the vertical electric field vector perpendicular to the QW) in the valence bands leading to improved polarization, lower optical losses, and lower threshold current. Note that the product of quantum-well thickness and strain must remain below a critical value. Above this value the layer experiences relaxation, causing a high number of defects and thus increased non-radiative recombination [56]. The separate confinement in diode lasers is achieved by pseudomorphic epitaxial growth of different compositions of III-V semiconductor compounds. The most commonly used epitaxial growth techniques for edge-emitting diode lasers are metal organic vapor phase epitaxy (MOVPE) and molecular beam epitaxy (MBE) as they deliver a good trade-off between crystal quality and deposition rate. A map of the most commonly used material compositions is shown in Figure 2.3. In particular the diode lasers within this work are fabricated based on various compositions of aluminum gallium arsenide ($Al_xGa_{1-x}As$) for the cladding and waveguide layers and indium aluminum gallium arsenide (InGaAs) for the quantum wells. The epitaxial layer structures are grown on GaAs substrates (cf. Figure 2.2 (b)) As shown in Figure 2.3, the refractive index of the $Al_xGa_{1-x}As$ layers varies with aluminum content without changing the lattice constant significantly, allowing for tailored optical confinement layers in



Dieses Werk ist copyrightgeschützt und darf in keiner Form vervielfältigt werden noch an Dritte weitergegeben werden.
Es gilt nur für den persönlichen Gebrauch.

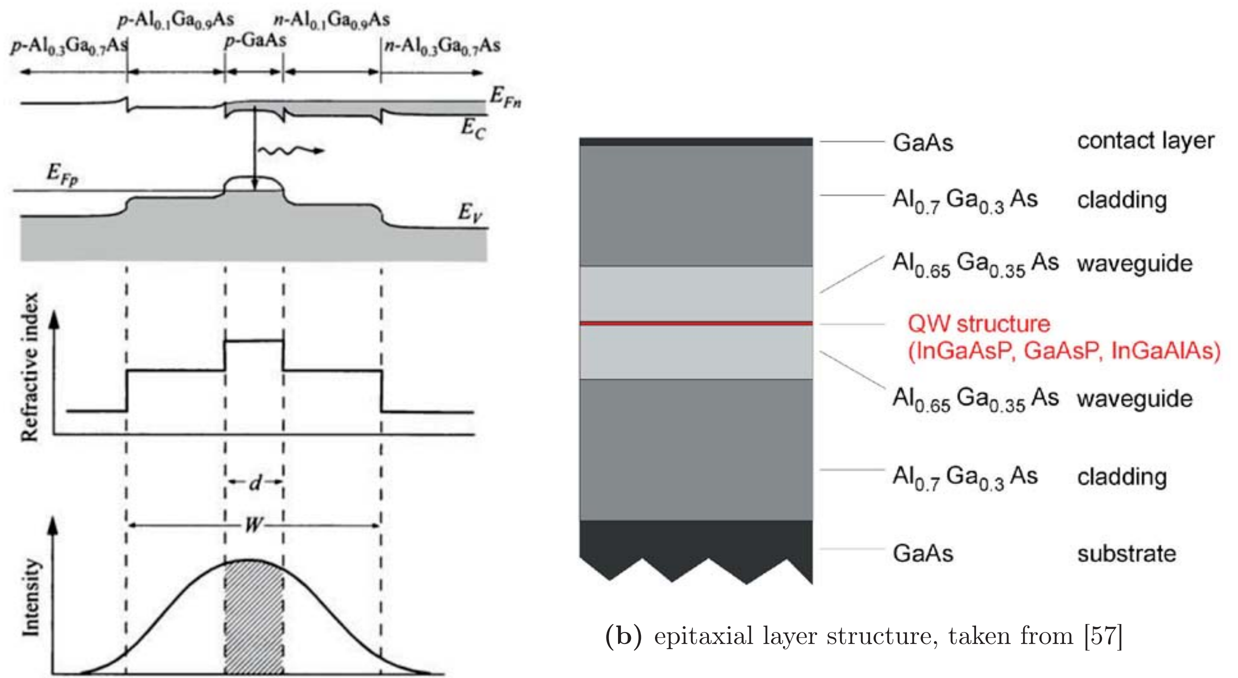


**(b)** epitaxial layer structure, taken from [57]

**(a)** band diagramm, refractive index and optical intensity profile (AlGaAs/GaAs), taken from [52]

**Fig. 2.2.:** Schematic depiction of a separate confinement heterostructure.

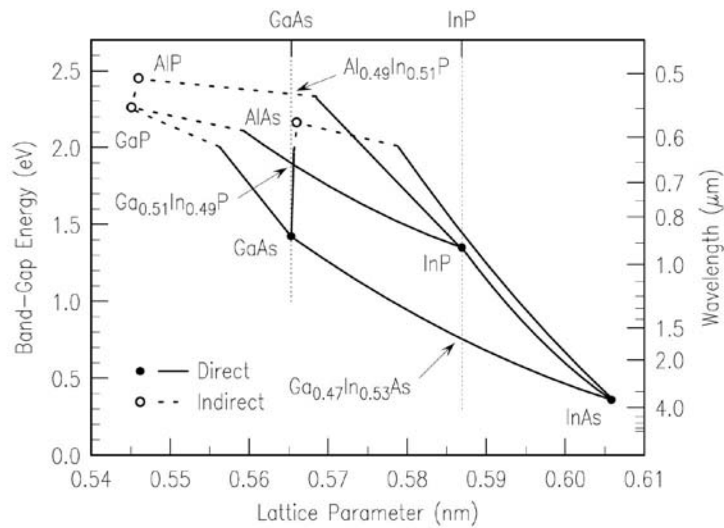


**Fig. 2.3.:** Band gap energy versus lattice constant for relevant III-V compound semiconductors for SCH based high-power diode lasers, taken from [56].



Dieses Werk ist copyrightgeschützt und darf in keiner Form vervielfältigt werden noch an Dritte weitergegeben werden.
Es gilt nur für den persönlichen Gebrauch.

vertical direction. InGaAs (as well as $Al_xGa_{1-x}As$ for $x \leq 0.45$) is a direct band gap material, allowing for efficient recombination within the quantum well. Further, in compressively strained quantum wells, light and heavy hole bands are split and the effective mass of the ligh holes in the valence band is reduced, implying a reduced density of states, Auger-recombination and intra-band absobrtion [59]. This effect enables a more efficient inversion within the quantum well and thus higher gain and lower threshold current. Additionally, strain management allows to tailor the spectral material gain (section 2.3) by changing the thickness of the quantum well.

### 2.1.1. Threshold gain and current

For edge emitting quantum well diode lasers the threshold gain and current is derived here. The obtained results are derived for Fabry-Pérot (FP) lasers but are also valid for distributed feedback (DFB) lasers when small adjustments are made. In FP-lasers with the cavity length $L$ the electrical field of a certain optical mode oscillates back and forth between the facets in longitudinal direction. The reflectivities of the facets with respect to the electrical field at the rear facet ($r_R$) and the front facet ($r_F$) define the amount of out-coupled light. Within the laser the electrical field is defined as

$$\underline{E}(x, y, z) = U(x, y) \exp(i(\omega t - \beta z))\underline{e_y} \tag{2.1}$$

with $\underline{e_y}$ being the unity vector in vertical direction indicating TE-polarization, $U(x, y)$ the transverse mode profile and

$$\beta = \frac{2\pi n_{eff}}{\lambda} + \frac{i}{2}(\Gamma g_{mod} + \alpha_i) \tag{2.2}$$

the propagation factor with the effective refractive index $n_{eff}$, the internal losses $\alpha_i$ and the modal gain $\Gamma g_{mod}$ referred to the overlap between optical field and active zone $\Gamma = \frac{V_{az}}{V_p}$. $V_{az}$ and $V_p$ are the occupied volume of active zone and photons, respectively. The threshold is reached when the electrical field reproduces itself after a full round-trip:

$$\underline{E}(z = 0) = r_R r_F \underline{E}(z = 2L)|^{\Gamma g_{mod} = \Gamma g_{th}} \tag{2.3}$$

Evaluating the real part of Equation 2.3 leads to the following expression for the threshold gain

$$\Gamma g_{th} = \alpha_i + \alpha_m \tag{2.4}$$

with the mirror losses

$$\alpha_m = \frac{1}{L} \ln\left(\frac{1}{r_R r_F}\right) \tag{2.5}$$

As the facet reflectivities are typically referred to the intensity ($R_R = r_R^2$ and $R_F = r_F^2$) it is more helpful to formulate the mirror losses as follows.

$$\alpha_m = -\frac{1}{2L} \ln(R_R R_F) \tag{2.6}$$



Dieses Werk ist copyrightgeschützt und darf in keiner Form vervielfältigt werden noch an Dritte weitergegeben werden.
Es gilt nur für den persönlichen Gebrauch.